

Design Of A Six Band Metamaterial Perfect Absorber Based On Honeycomb-Shape In The Terahertz Frequency Range

Djekinnou D. Daniel E, Prof. Zhang GuoPing

Abstract: We proposed the model of a terahertz metamaterial absorber composed of metallic honeycomb cells joined by a cross in the center, a dielectric layer and a metallic substrate. The simulation shows that the designed metamaterial absorber has six distinct absorption peaks at 18.306; 19.836; 26.211; 28.302; 29.628 and 34.762 Terahertz with absorption rates of 97%; 98.6%; 99.3%; 97.7%; 99.8% and 94.3% respectively. The angular study of the system revealed that it remains a high absorption metamaterial absorber under both transverse electric and magnetic configurations.

Index Terms: metamaterial; perfect absorber; six-band; terahertz.

1. INTRODUCTION

Metamaterial absorbers are artificial and homogeneously engineered electromagnetic structures made of materials existing in nature but which exhibit unusual and unique properties that do not exist in the nature [1]. The unique properties of metamaterial absorbers offer them great potentials in many applications such as sensing, antennas, filters, solar cells and energy harvesting[2], [3]. Electromagnetic absorbers have been around since 1952 [4] but the first near unity metamaterial absorber was proposed in 2008 [5]. Since then, several metamaterial absorbers of various designs have been proposed. The proposed metamaterial absorbers perform at various range of the microwave, infrared and terahertz frequency regimes. If some of the metamaterials absorbers focus on single and dual-bands [6], [7], [8], [9], it has been noticed that some recent works focus on triple-bands perfect metamaterial absorbers [10],[11],[12],[13],[14],[15] while others on more than triple to broadband metamaterial perfect absorbers [16],[17],[18]. In this study, we proposed a six band perfect metamaterial absorber based on two strip lines forming a plus sign structure whose four ends are connected to honeycombs. One end of each honeycomb has been flattened to perfectly join the plus structure.

2. STRUCTURE DESIGN

Fig 1 shows a schematic representation of the proposed metamaterial perfect absorber. It consists of a gold top layer which is separated from the copper substrate layer by a quartz dielectric layer. In the study, copper is considered as a pure lossy metal with an electrical conductivity $\sigma = 5.96e + 07 [s/m]$. The permittivity of the quartz substrate is $\epsilon_i = 3.75$. With all proportions in μm , the optimized geometrical parameters of the unit cell of the proposed perfect metamaterial absorber are as follows: $w=0.22$ $l=3$; $L1=4$; $d=4.7$; $g=0.522$; $S=0.475$; $a=12$. The optimized proportions make the proposed metamaterial

absorber perfect since its absorption coefficients are almost unity.

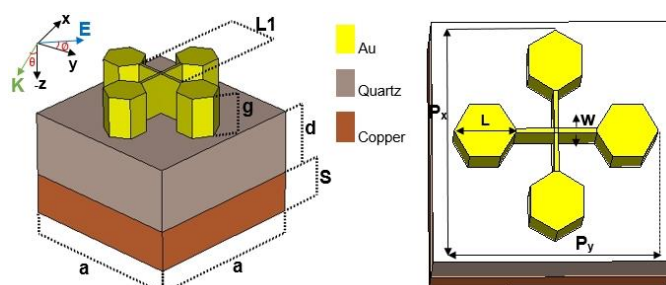


Fig 1. Schematic representation of the six-band perfect metamaterial absorber. The geometric parameters of the plus sign structure are $L1=4$; $w=0.22$. The geometric parameters of a honeycomb are $L=3$; $w=0.22$. The length of the unit cell is $a=12$. The thickness of the copper substrate is $s=0.475$ while that of the quartz dielectric layer is $d=4.7$. The height of the plus sign structure and the honeycombs is $g=0.522$. The periods of the structure (honeycombs and plus sign structure) are $P_x = P_y$ and are all dependent of L .

The complete analysis of the metamaterial absorber has been conducted using CST 3-D simulation software. In the process, unit cell along x and y axis and open boundaries conditions to Z axis have been applied along with floquet port excitation. Mathematically, the absorptivity of an absorber can be computed as $A = 1 - R - T$ or $A = 1 - |S_{11}|^2 - |S_{21}|^2$ where $R = |S_{11}|^2$ is the reflected power and $T = |S_{21}|^2$ the transmitted power. For a perfect metamaterial absorber, the transmitted power is negligible resulting in $A = 1 - |S_{11}|^2$. This is due to the presence of the copper layer at the bottom of the quartz material which restricts the transmission of the incident electromagnetic wave.

3. RESULTS AND DISCUSSION

Fig 2 shows the absorption, the transmission and the reflection curves of the proposed MMA.

- Djekinnou D. Daniel E. is currently pursuing PhD. degree program in optical engineering in Central China normal University, China. E-mail: dedd8@yahoo.fr
- Zhang Guoping is currently a professor in the College of Physical Science and Technology at Central China Normal University. E-mail: 19634067@qq.com

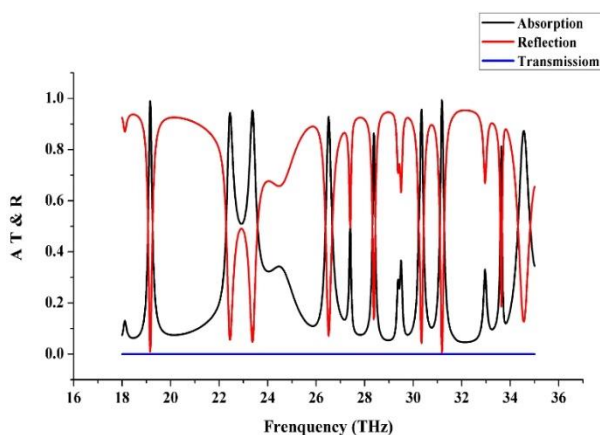


Fig 2. Absorption, Transmission and Reflection spectra with constant parameters: $L=4$; $w=0.22$; $L=3$; $a=12$; $s=0.475$; $d=4.7$ and $g=0.522$.

The designed MMA (metamaterial absorber) has six distinctive resonance peaks at the frequencies of $f_1 = 18.306$ THz; $f_2 = 19.836$ THz; $f_3 = 26.211$ THz; $f_4 = 28.302$ THz; $f_5 = 29.628$ THz and $f_6 = 34.762$ THz. Each of the resonances has respectively an approximate absorption of 97%; 98.6%; 99.3%; 97.7%; 99.8%; 94.3%. It is demonstrated through numerical simulation that the average absorption peak at six resonances is 97.78. Mathematically, the Q factor is expressed as $Q = \frac{f_0}{FWHM}$ where f_0 is the central frequency and FWHM the full width at half maximum [19]. The half width half maximum of the resonance absorption peak for our design is about 0.156; 0.129; 0.177; 0.154; 0.153; 0.272. The corresponding Q factor is hence about $Q_1 = 117.35$; $Q_2 = 153.78$; $Q_3 = 148.08$; $Q_4 = 183.78$; $Q_5 = 193.65$ and $Q_6 = 127.80$ respectively. The proposed MMA has a significantly higher Q factor compare to the previously proposed MMA [17]; [18]; [19]. Fig 3 shows the dependence of the absorption resonances to the honeycomb length. During this sweep, all the other parameters were kept constant. It is observed that an increase of L from $3\mu\text{m}$ to $3.2\mu\text{m}$ causes a relatively small shift in the percentage of the absorption peaks and their frequencies of appearance. We noticed a strong shift from 97% of absorption at 18.306 THz to 99.8% of absorption at 18.55THz. From 98.6% at 19.836 THz, the absorption peak shifted to 99.3% at 19.87THz. A major shift was also noticed when $L=3.4\mu\text{m}$. It was noticed that f_1 shifted from 18.306THz with 97% of absorption to 18.17THz with 99.8%. The major shift noticed for $L=2.8\mu\text{m}$ is at $f=34.745$ THz. Compared to $L=3\mu\text{m}$ which has an absorption rate of 94.3% at 34.762THz, we obtained an absorption rate of 99.8% at $f=34.745$ THz. We also have a resonance at $f=23.321$ THz with 96.2% of absorption. At $L=2.4\mu\text{m}$, three major resonance shifts have been noticed at 18.255THz, 19.87THz and 28.234THz. These frequencies have an absorption rate of 99.8%, 99.3% and 97.3% respectively. It results from the previous analysis that the proposed perfect metamaterial absorber has strong confinement around 18THz, 19THz, 26THz, 28THz and 34.762THz.

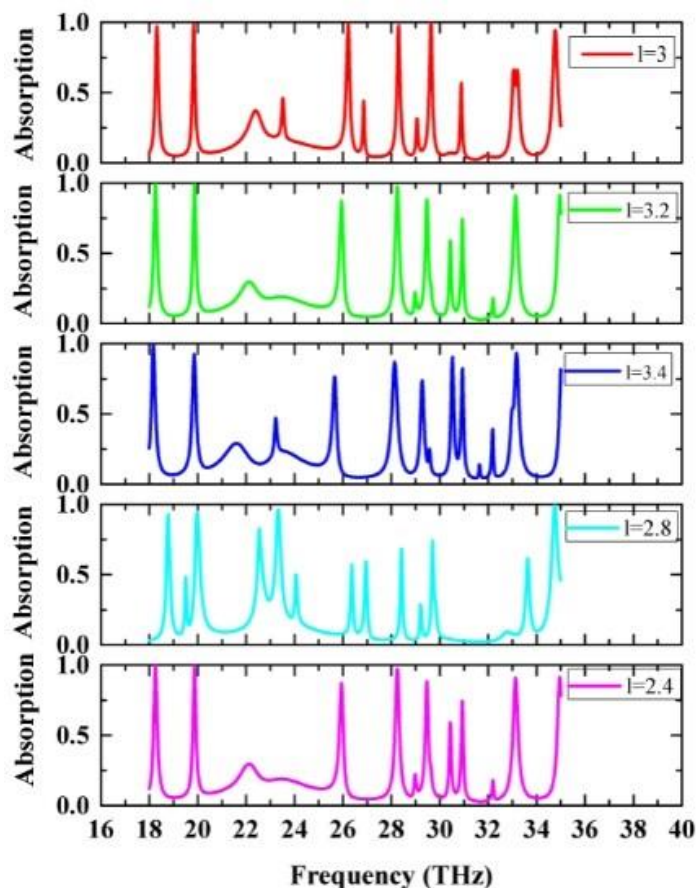


Fig 3. Absorption spectra for l sweep. (a) $L=3\mu\text{m}$; (b) $L=3.2\mu\text{m}$; (c) $L=3.8\mu\text{m}$; (d) $L=2.8\mu\text{m}$; (e) $L=2.4\mu\text{m}$.

4. SURFACE CURRENT AND E-FIELD DISTRIBUTIONS STUDY

The surface current distributions are depicted in **Error! Reference source not found.** **Error! Reference source not found.** illustrate respectively the current distribution at the top layer at 18.306THz, 19.836 THz, 26.211 THz, 28.302 THz, 29.628 THz and 34.762 THz. Similarly, **Error! Reference source not found.** illustrate the current distribution at the bottom layer of the proposed MMA. It can be observed that at all peaks, the combination of all the surface current on both top and bottom form a circulating current. This anti-parallel flow of current in the MMA causes the occurrence of a strong magnetic excitation which results in the observed peaks. Reciprocally, **Error! Reference source not found.** illustrates the electric field distribution at all six absorption peaks. In all cases, the electric field seems to be evenly distributed on the component of the MMA. At $f=18.306$ THz i.e. **Error! Reference source not found.**, the electric field is more accentuated on the inner contour of the two vertical honeycombs. This scenario describes also what happens at $f=29.628$ THz and $f=34.762$ THz i.e. **Error! Reference source not found.** and **Error! Reference source not found.** respectively. At $f=19.836$ THz, $f=26.211$ THz and $f=28.302$ THz i.e. **Error! Reference source not found.**; **Error! Reference source not found.** and **Error! Reference source not found.** respectively, the electric field is located on all four honeycombs but its maximum concentration is located on the horizontal components of the structure.

Top layer

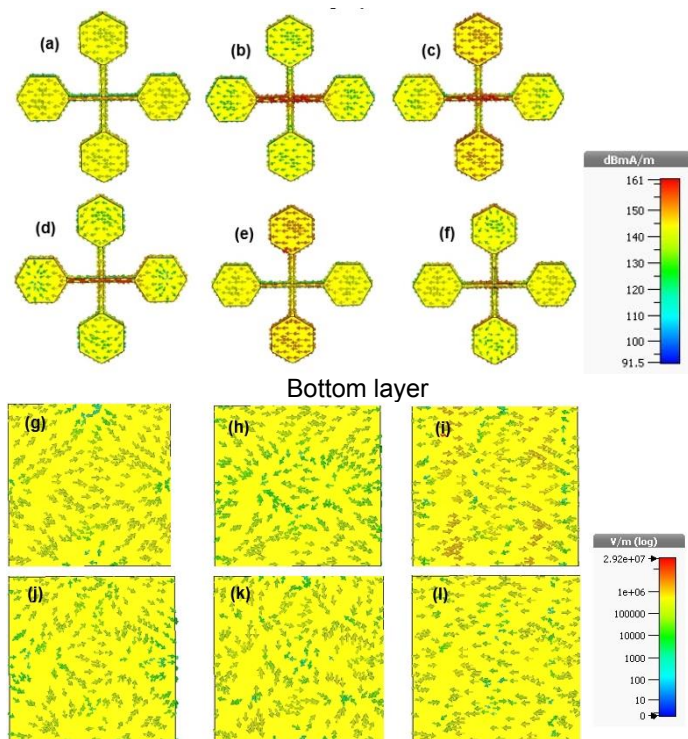


Fig 4. Surface current distribution plot of the proposed perfect metamaterial absorber for $l=3\mu\text{m}$, (a) $f=18.306\text{THz}$; (b) $f=19.836\text{THz}$; (c) $f=26.211\text{THz}$; (d) $f=28.302\text{THz}$; (e) $f=29.628\text{THz}$; (f) $f=34.762\text{THz}$ top layer and (g)-(l) bottom layer respectively.

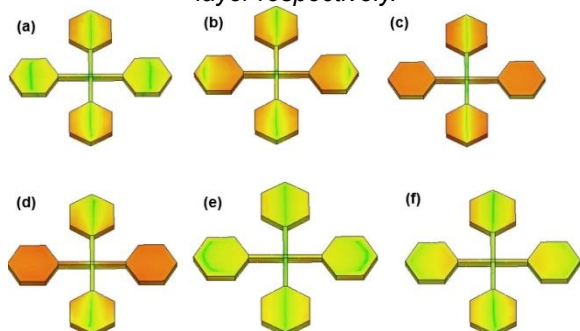


Fig 5. Electric field distribution plot at all six absorption peak frequencies of the suggested six band absorber for $l=3\mu\text{m}$; (a) $f=18.306\text{THz}$; (b) $f=19.836\text{THz}$; (c) $f=26.211\text{THz}$; (d) $f=28.302\text{THz}$; (e) $f=29.628\text{THz}$; (f) $f=34.762\text{THz}$.

5. POLARIZATION AND ANGULAR STABILITY

Fig 6 presents the absorptivity of the proposed MMA based on different polarization angles ϕ . The study reveals that from $\phi = 0^\circ$ to $\phi = 30^\circ$, the resonance frequencies of the proposed structure remain invariable despite the change in the absorption values. From $\phi = 0^\circ$ to $\phi = 15^\circ$, major variations are noticed at $f=26.211\text{ THz}$ where the absorptivity increased from 99.3% to 99.9%, from 99.8% to 99.9% and from 94.3% to 94.8%. These major variations are explained through the study of the normal component of the e-field distribution at $f=26.211\text{THz}$ for $\phi = 0^\circ$ and $\phi = 15^\circ$. As illustrated in Fig 7 at resonance for $\phi = 15^\circ$, we have a better distribution of the e-field as compared to $\phi = 0^\circ$ i.e. Fig 7(b). This results in more power being absorbed for $\phi = 15^\circ$. The increase variations could also be explained by the presence of standing waves within the MMA interfering

constructively for $\phi = 15^\circ$ [20].

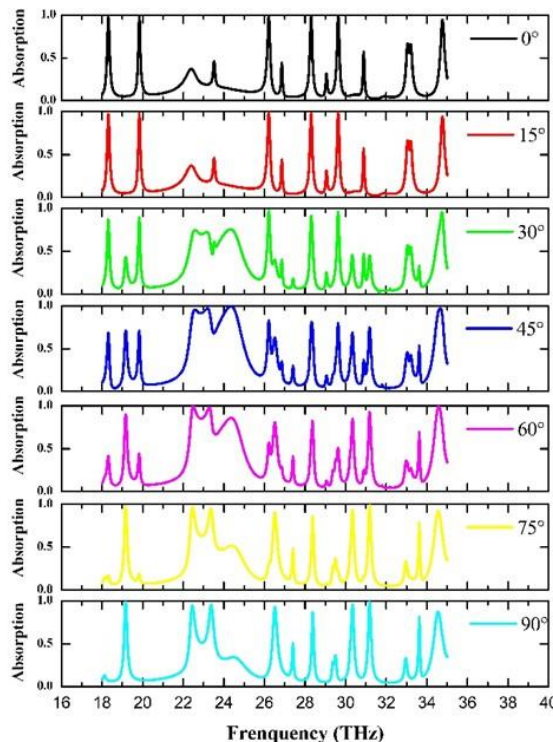


Fig 6. The absorption curves of the proposed MMA under various polarization angles ϕ .

At $\phi = 30^\circ$, the resonance frequency of $f=34.762\text{THz}$ has shifted to 34.745 THz with an absorptivity of 94.3% and 95.4% respectively.

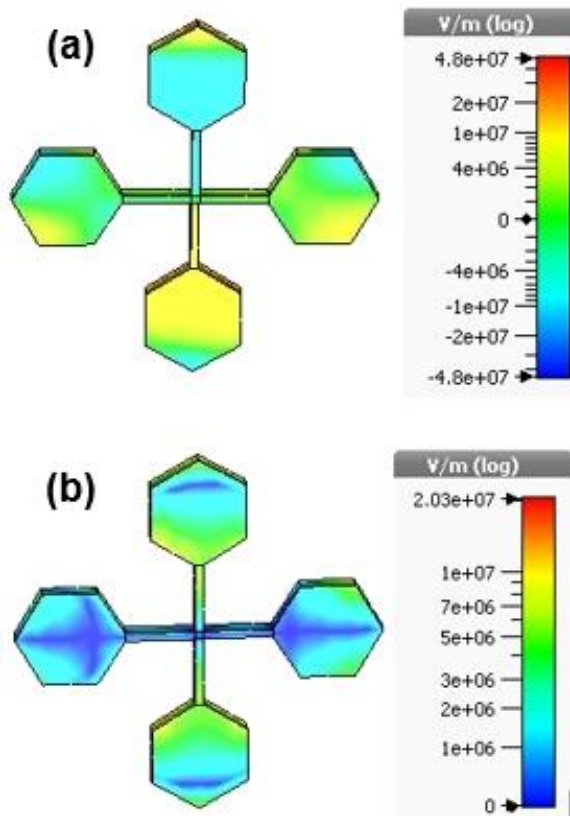


Fig 7. Normal component illustration of e-field distribution at

$f=26.211$ THz for (a) $\theta = 15^\circ$ and (b) $\theta = 0^\circ$.

TABLE 1 FREQUENCIES (f) AND RESPECTIVE ABSORPTION (A) PEAKS RESULT FROM POLARIZATION

θ	f in THz	A	θ	f in THz	A
45°	22.573	95	60°	22.488	99.8
	23.202	97		23.287	98
	24.341	99.6		31.175	92
	34.66	97		34.575	99.47
75°	19.156	97.5	90°	19.156	98.9
	22.454	96.63		22.454	94
	23.355	95		23.372	95.2
	30.342	93		26.517	92.2
	31.175	98.7		30.342	95.7
	34.558	92.2		31.175	99.4

As the polarization angle increases, new peaks with over 90% of absorption have been observed. They are summarized in the table above. To further study the proposed MMA, we investigated its angular dependency for both TE and TM configuration at various incident angles. The results are shown in **Error! Reference source not found.** and **Error! Reference source not found.**. At $\theta = 0^\circ$, the absorption spectra remains invariable under both polarizations. The study reveals that most of the absorbance peaks are above 90% at the different incident angles. It results that, the incident angle and the light polarization do not to a large extent affect the high absorption property of the proposed MMA. Occurrences of new absorption peaks were also noticed. More interesting, under both configurations, we obtained seven to eight absorption peaks at various incident angles. At $\theta = 45^\circ$ under TM configuration, we have obtained eight absorption peaks of over 98% of absorption. Under both configuration, seven absorption peaks of over 97% of absorption were obtained at $\theta = 75^\circ$. The high absorption of the proposed MMA despite the increment of the incident angle is due to the geometry of the system. Indeed, the repartition of the honeycombs cells allows the MMA to receive enough radiation which allows a high surface current density and as stated earlier, the anti-parallel flow of current in the MMA causes the occurrence of a strong magnetic excitation which results in the observed peaks.

various incident angles θ (0–75 degrees) for (a) TM polarized, (b) TE polarized.

CONCLUSION

In summary, we have proposed a six band perfect metamaterial absorber metallic honeycombs cells join by a plus sign structure in the center. The numerical simulation proved that the proposed MMA at six resonances has an average absorption of 97.78%. It has further been noticed that, the geometry of the proposed MMA allows it to receive important energy from the incident wave in both TE and TM configuration allowing it to keep it high absorption efficiency. The angular study of the MMA shows that with further geometrical scalability, the MMA could achieved broadband frequency absorption due to the closeness of some absorption peaks frequency.

REFERENCES

- [1] M. B. Ghandehari, N. Feiz and A. Akbar Khazaei, Polarization and wide angle independent perfect metamaterial triple band absorber based on hexagonal shapes, International Journal of Applied Electromagnetics and Mechanics 48 (2015) 77–83 DOI 10.3233/JAE-140180.
- [2] S. Jamilan¹, Mohammad N. Azarmanesh¹, and D. Zari, Design and Characterization of a Dual-Band Metamaterial Absorber Based on Destructive Interferences, Progress In Electromagnetics Research C, Vol. 47, 95{101, 2014.
- [3] N. Mishra* and R. K. Chaudhary, Design and Development of an Ultrathin Triple Band Microwave Absorber Using Miniaturized Metamaterial Structure for Near-Unity Absorption Characteristics, Progress In Electromagnetics Research C, Vol. 94, 89–101, 2019
- [4] Salisbury, W. W., "Absorbent body for electromagnetic waves," U.S. Patent 2599944, filled May 11, 1943, granted June 10, 1952.
- [5] Landy NI, Sajuyigbe S, Mock JJ, Smith DR, Padilla WJ. Perfect metamaterial absorber, Phys Rev Lett 2008;100:207402.
- [6] Y. Ming Qing¹, H. Feng Ma¹, S. Yu and T. Jun Cui, Tunable dual-band perfect metamaterial absorber based on a graphene-SiC hybrid system by multiple resonance modes, Journal of Physics D: Applied Physics, 2018.
- [7] W. Zhu , X. Zhao , B. Gong, L. Liu and Bin Su, Optical metamaterial absorber based on leaf-shaped cells, Appl Phys A (2011) 102: 147–151
- [8] N. Zhang, P. Zhou, D. Cheng, X. Weng, J. Xie, and L. Deng, Dual-band absorption of mid-infrared metamaterial absorber based on distinct dielectric spacing layers, OPTICS LETTERS, April 1, 2013 / Vol. 38, No. 7.
- [9] J. Hao, J. Wang, X. Liu, W. J. Padilla, L. Zhou et al., High performance optical absorber based on a plasmonic metamaterial APPLIED PHYSICS LETTERS 96, 251104_2010.
- [10] C. Cena,c, Z. Yia, G. Zhangb, Y. Zhanga, C. Lianga, X. Chena, Y. Tanga, X. Yed, Y. Yie, J. Wangf and J. Huag, Theoretical design of a triple-band perfect metamaterial absorber in the THz frequency range, Results in Physics, 2019.
- [11] K. Muthukrishnan and V. Narasimhan, An Ultra-Thin Triple-Band Polarization-Independent Wide-Angle Microwave Metamaterial Absorber, Springer Science+Business Media, LLC, part of Springer Nature 2019.
- [12] Z. Yia, H. Lina , G. Niuc, X. Chena, Z. Zhoua, X. Yec et al, Graphene-based tunable triple-band plasmonic perfect metamaterial absorber with good angle-polarization-tolerance, Results in Physics 13 (2019) 102149.
- [13] X. Shen, Y. Yang, Y. Zang, J. Gu, J. Han, W.i Zhang, and T. Jun

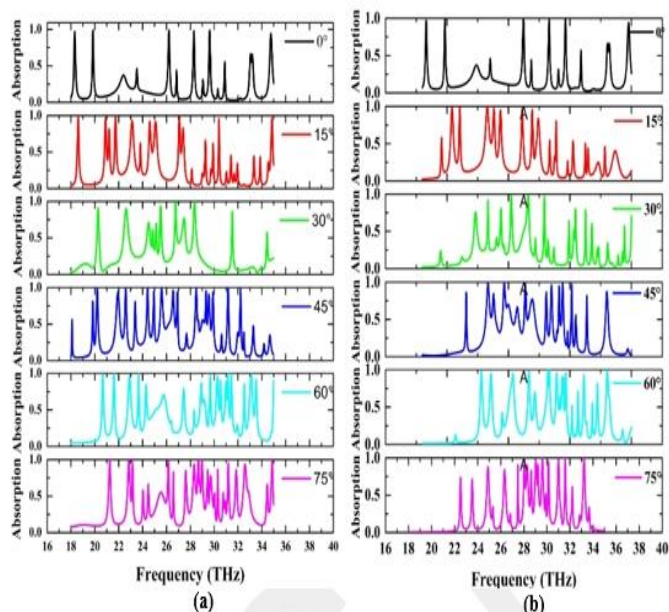


Fig 8. The absorption curves of the proposed MMA under

- Cui, Triple-band terahertz metamaterial absorber: Design, experiment, and physical interpretation, *APPLIED PHYSICS LETTERS* 101, 154102 (2012).
- [14] M. Bahdorzadeh Ghandehari, N. Feiz and A. Akbar Khazaei, Polarization and wide angle independent perfect metamaterial triple band absorber based on hexagonal shapes, *International Journal of Applied Electromagnetics and Mechanics* 48 (2015) 77–83
- [15] X. Shen, T. J. Cui, J. Zhao, H. Feng Ma, W. Xiang Jiang,1 and H. Li1, Polarization-independent wide-angle triple-band metamaterial absorber, *Optical Society of America*, 2011.
- [16] Chen X-li, Tian C-hui, Che Z-xin, Chen T-ping, Selective metamaterial perfect absorber for infrared and 1.54_μ laser compatible stealth technology, *Optik* (2018), <https://doi.org/10.1016/j.ijleo.2018.07.091>
- [17] H. Zou, Y Cheng, Design of a six-band terahertz metamaterial absorber for temperature sensing application, *Optical Materials* 88 (2019) 674–679.
- [18] D. Wu, C. Liu, Y. Liu, Z. Xu, Z. Yu, L. Yu et al., Numerical study of a wide-angle polarizationindependent ultra-broadband efficient selective metamaterial absorber for near-ideal solar thermal energy conversion, *RSC Adv.*, 2018, 8, 21054–21064.
- [19] Y. Zhi Cheng , M. Lin Huang , H. Ran Chen , Z. Zhong Guo , X. Song Mao and R. Zhou Gong , Ultrathin Six-Band Polarization-Insensitive Perfect Metamaterial Absorber Based on a Cross-Cave Patch Resonator for Terahertz Waves, *Materials* 2017, 10, 591; doi:10.3390/ma10060591
- [20] K.G. Ayappa (1999) Resonant Microwave Power Absorption in Slabs, *Journal of Microwave Power and Electromagnetic Energy*, 34:1, 33-41, DOI: 10.1080/08327823.1999.11688386